JOURNAL OF GUIDANCE, CONTROL, AND DYNAMICS
Vol. 26, No. 1, January–February 2003

Third-Body Perturbation in Orbits Around Natural Satellites

Antonio Fernando Bertachini de Almeida Prado
National Institute for Space Research, 12227-010 São José dos Campos, Brazil

An analytical and a numerical study of the perturbation imparted to a spacecraft by a third body is developed. There are several important applications of the present research, such as calculation of the effect of lunar and solar perturbations on high-altitude Earth satellites. The goal is to study the evolution of orbits around some important natural satellites of the solar system, such as the moon, the Galilean satellites of Jupiter, Titan, Titania, Triton, and Charon. There is special interest in learning under which conditions a near-circular orbit remains near circular. The existence of circular, equatorial, and frozen orbits are also considered for a lunar satellite, but the results are valid for any system of primaries by making a time transformation that depends on the masses of the bodies involved. Several plots will show the time histories of the Keplerian elements of the orbits involved. Then, a study is performed to estimate the lifetime of orbits around those natural satellites.

Introduction

THE majority of papers that considered the third-body perturbation problem studied the perturbation due to the sun and the moon in a satellite in orbit around the Earth. Kozai[1] developed the main secular and long-period terms of the disturbing function due to the lunisolar perturbations in terms of the orbital elements of the satellite, the sun, and the moon. This research would later be expanded by Musen et al.[2] to include the parallactic term in the disturbing function. After that, Kozai[3] studied the problem of secular perturbations in asteroids with high inclination and eccentricity, considering that they are perturbed by Jupiter, which is assumed to be in a circular orbit around the sun. Blitzer[4] obtained estimates of the lunisolar disturbances using methods of classical mechanics, but only for the secular terms. Following that, Cook[5] used Lagrange's planetary equations to obtain expressions for the variation of elements during a revolution of the satellite and for the rate of variation of the same elements. In that same year, Kaula[6] derived general terms of the disturbing function for the lunisolar perturbation, using equatorial elements for the moon, but the terms did not supply a definitive algorithm for the calculations. Again, Kozai[7] approached that problem and included indirect terms of the disturbance due to the alteration of the terrestrial flattening due to those forces.

In the 1970s, that subject was studied again. Giacaglia[8] obtained the disturbing function for the disturbance of the moon using ecliptic elements for the moon and equatorial elements for the satellite. Secular-, long-, and short-period terms were calculated and expressed in a closed form. Kozai[9] developed an alternative method for the calculation of the lunisolar disturbances. The disturbing function was expressed in terms of the orbital elements of the satellite and the polar geocentric coordinates of the sun and the moon. The secular- and long-period terms are derived by numerical integration and the short-period terms are obtained analytically.

In the following decade, Hough[10] studied the effects of the lunisolar disturbance in orbits close to the inclinations 63.4 and 116.6 deg (critical inclinations with respect to the geopotential of the Earth) and concluded that the effects are significant in high altitudes.

All of the preceding references represent fundamental contributions in the subject, and they possess an analytic focus, dedicated to the derivation of equations. In the present work, a more practical approach is used with the idea of complementing the existent literature. Some recent studies have provided numeric comparisons.

In this paper, several topics related to this problem will be studied. In particular, the so-called critical angle of the third-body perturbation, which is a value for the inclination such that any near-circular orbit with inclination below this remains near circular, is discussed in detail for a lunar satellite. The assumptions of our model are similar to the ones made in the restricted three-body problem.

1) There are only three bodies involved in the system: one body with mass m_0 fixed at the origin of the reference system, a massless spacecraft in a elliptic three-dimensional orbit around this body, and a third body in a circular orbit around this same central body in the plane x–y.

2) The motion of the spacecraft is assumed to be a three-dimensional Keplerian orbit with its orbital elements disturbed by the third body.

The motion of the spacecraft is studied under the double-averaged analytical model with the disturbing function expanded in Legendre polynomials up to fourth order and as the full restricted problem. The double average is taken over the mean motion of the satellite and over the mean motion of the disturbing body. That modern computers can easily integrate numerical trajectories using complex models for the dynamics does not invalidate the use of models based in analytical approximations. The most important reason for this is that a double-averaged model, like the one shown here, can eliminate short-period periodic perturbations that appear in the trajectories. In that way, smooth curves that show the evolution of the mean orbital elements for a long time period can be constructed. These provide a better understanding of the physical phenomenon studied

Dr. Antonio F. B. A. Prado is the Academic Coordinator and Professor of the Aerospace Engineering Graduate School at the National Institute for Space Research (INPE) in Brazil. He was born in Jau, Brazil. He received the following academic degrees: Ph.D. (1993) and M.S. (1991) in aerospace engineering from the University of Texas at Austin, M.S. in space science (1989) from INPE, and B.S. in physics (1986) and chemical engineering (1985) from the University of Sao Paulo (Brazil). He is member of the Tau-Beta-Pi National Engineering Honor Society and of the Honor Society of Phi-Kappa-Phi. Dr. Prado is an Associate Fellow of the AIAA.

Received 8 February 2000; revision received 18 September 2000; accepted for publication 20 November 2000.

and allow the study of long-term stability of the orbits in the presence of disturbances that cause slow changes in the orbital elements. Note that the truncated equations of motion could be numerically integrated much faster than the full equations of the restricted three-body problem. The next sections present the mathematical models used; the study of circular, near-circular, equatorial, and frozen orbits; and the study of the lifetime of orbits around natural satellites of the solar system.

Mathematical Models

This section derives the equations required by the mathematical models used during the simulations made in this research. It is assumed that the main body with mass m_0 is fixed in the center of the reference system x–y. The perturbing body with mass m' is in a circular orbit with semimajor axis a' and mean motion n' (given by the expression $n'^2a'^3 = G[m_0 + m']$). The massless spacecraft is in an elliptic three-dimensional orbit with orbital elements: a (semimajor axis), e (eccentricity), i (inclination), ω (argument of periapsis), Ω (longitude of the ascending node), and n (the mean motion) given by the expression $n^2a^3 = Gm_0$. In this situation, the disturbing potential that the spacecraft has from the action of the disturbing body is given by

$$R = \frac{\mu' G(m_0 + m')}{\sqrt{r^2 + r'^2 - 2rr'\cos(S)}} \tag{1}$$

where $\mu' = m'/(m_0 + m')$, G is the gravitational constant, and S is the angle between the line that connects the massive central body and the perturbed body (the spacecraft) and the line that connects the massive central body and the perturbing body (the third body).

With the traditional expansion in Legendre polynomials (assuming that $r' \gg r$), the following expression can be found:

$$R = \frac{\mu' G(m_0 + m')}{r'} \sum_{n=2}^{\infty} \left(\frac{r}{r'}\right)^n P_n[\cos(S)] \tag{2}$$

where P_n are the Legendre polynomials.

For the models used in this research, it is necessary to calculate the parts of the disturbing function due to P_2, P_3, and P_4 (R_2, R_3, and R_4, respectively). They are

$$R_2 = \frac{\mu' G[m_0 + m']}{r'} \left\{ \left(\frac{r}{r'}\right)^2 P_2[\cos(S)] \right\}$$

$$= \frac{\mu' n'^2 a^2}{2} \left(\frac{a'}{r'}\right)^3 \left(\frac{r}{a}\right)^2 [3\cos^2(S) - 1] \tag{3}$$

$$R_3 = \frac{\mu' G[m_0 + m']}{r'} \left\{ \left(\frac{r}{r'}\right)^3 P_3[\cos(S)] \right\}$$

$$= \frac{\mu' n'^2 a^3}{2r'} \left(\frac{a'}{r'}\right)^3 \left(\frac{r}{a}\right)^3 [5\cos^3(S) - 3\cos(S)] \tag{4}$$

$$R_4 = \frac{\mu' G[m_0 + m']}{r'} \left\{ \left(\frac{r}{r'}\right)^4 P_4[\cos(S)] \right\}$$

$$= \frac{\mu' n'^2 a^4 a'^3}{8r'^5} \left(\frac{r}{a}\right)^4 [35\cos^4(S) - 30\cos^2(S) + 3] \tag{5}$$

A substitution using the expression $n'^2a'^3 = G[m_0 + m']$ was made between the first and the second member of those equations. The next step is to average those quantities over the short period of the satellite as well as with respect to the distant perturbing body. The standard definition for average used in this research is

$$\langle F \rangle = \frac{1}{2\pi} \int_0^{2\pi} (F)\, \mathrm{d}M$$

where M is the mean anomaly, which is proportional to time.

To perform the average over R_2, R_3, and R_4, one proceeds as follows. First define the quantities $\alpha = \hat{P} \cdot \hat{r}'$ and $\beta = \hat{Q} \cdot \hat{r}'$, where $\hat{r}'$ is the unit vector pointing from the central body to the disturbing body and $\hat{P}$ and $\hat{Q}$ are the usual orthogonal unit vectors, functions of i, ω, and Ω in the plane of the satellite orbit, with $\hat{P}$ pointing toward the periapsis. For the special case considered here of circular orbits for the disturbing body, the following relations are available:

$$\alpha = \cos(\omega)\cos(\Omega - M') - \cos(i)\sin(\omega)\sin(\Omega - M') \tag{6}$$

$$\beta = -\sin(\omega)\cos(\Omega - M') - \cos(i)\cos(\omega)\sin(\Omega - M') \tag{7}$$

With this definition and the geometry involved, it is possible to relate the angle S to the positions of the perturbing and perturbed bodies. This can be made by the equation (where f is the true anomaly of the satellite)

$$\cos(S) = \alpha\cos(f) + \beta\sin(f) \tag{8}$$

Then, combining Eq. (8) with Eqs. (3–5), the perturbing potential becomes a function of the orbital elements of the satellite. Next, it is necessary to replace the true anomaly f with the eccentric anomaly E. This is made by the well-known relations $\sin(f) = [\sqrt{(1-e^2)}\sin(E)]/[1 - e\cos(E)]$, $\cos(f) = [\cos(E) - e]/[1 - e\cos(E)]$, and $r/a = 1 - e\cos(E)$. Then, the integrations required to obtain the averages are realized in terms of the eccentric anomaly, not in terms of the mean anomaly. To do that, the relation $\mathrm{d}M = [1 - e\cos(E)]\,\mathrm{d}E$ is also used.

After this process, the following identities appear:

$$\langle (r/a)^2\cos^2(f)\rangle = (1 + 4e^2)/2, \qquad \langle (r/a)^2\cos(f)\sin(f)\rangle = 0$$

$$\langle (r/a)^2\sin^2(f)\rangle = (1 - e^2)/2, \qquad \langle (r/a)^2\rangle = (2 + 3e^2)/2$$

$$\langle (r/a)^3\cos(f)\rangle = -[5e(4 + 3e^2)/8]$$

$$\langle (r/a)^3\cos^3(f)\rangle = -[5e(3 + 4e^2)/8]$$

$$\langle (r/a)^3\sin(f)\rangle = 0, \qquad \langle (r/a)^3\cos^2(f)\sin(f)\rangle = 0$$

$$\langle (r/a)^3\cos(f)\sin^2(f)\rangle = 5e(e^2 - 1)/8, \qquad \langle (r/a)^3\sin^3(f)\rangle = 0$$

$$\langle (r/a)^4\cos^4(f)\rangle = 3(1 + 12e^2 + 8e^4)/8$$

$$\langle (r/a)^4\cos^3(f)\sin(f)\rangle = 0$$

$$\langle (r/a)^4\cos^2(f)\sin^2(f)\rangle = (1 + 5e^2 - 6e^4)/8$$

$$\langle (r/a)^4\cos(f)\sin^3(f)\rangle = 0, \qquad \langle (r/a)^4\sin^4(f)\rangle = 3(e^2 - 1)^2/8$$

$$\langle (r/a)^4\cos^2(f)\rangle = (4 + 41e^2 + 18e^4)/8$$

$$\langle (r/a)^4\cos(f)\sin(f)\rangle = 0, \qquad \langle r/a)^4\sin^2(f)\rangle = (4 - e^2 - 3e^4)/8$$

$$\langle (r/a)^4\rangle = (8 + 40e^2 + 15e^4)/8$$

After using those quantities, expressions (3–5) become

$$\langle R_2\rangle = \frac{\mu' a^2 n'^2}{2} \left(\frac{a'}{r'}\right)^3 \left\{ \left(1 + \frac{3}{2}e^2\right) \left[\frac{3}{2}(\alpha^2 + \beta^2) - 1\right] + \frac{15e^2}{4}(\alpha^2 - \beta^2) \right\} \tag{9}$$

$$\langle R_3\rangle = \frac{\mu' a^3 n'^2}{2a'} \left(\frac{a'}{r'}\right)^4 \left[\frac{15\alpha e(4 + 3e^2)}{8} - \frac{25\alpha^3 e(3 + 4e^2)}{8} + \frac{75\alpha\beta^2 e(e^2 - 1)}{8} \right] \tag{10}$$

$$\langle R_4\rangle = \frac{3\mu' a'^3 n'^2 a^4}{64r'^5} [(8 + 40e^2 + 15e^4) - 10\alpha^2(4 + 41e^2 + 18e^4) + 35\alpha^4(1 + 12e^2 + 8e^4) - 10\beta^2(4 - e^2 - 3e^4) + 70\alpha^2\beta^2(1 + 5e^2 - 6e^4) + 35\beta^4(e^2 - 1)^2] \tag{11}$$

Next, one takes the second average with respect to the disturbing body to eliminate the variable M'. To do this, it is necessary to hold the Keplerian elements of the spacecraft constant during the process of averaging. This is possible due to the hierarchy of timescales: the period of satellite is much less than the period of disturbing body, which is much less than the period of slow oscillations in the orbital elements. After making these assumptions, the following identities, always valid for circular orbits only, are obtained:

$$\langle\alpha\rangle = \langle\alpha^3\rangle = \langle\alpha\beta^2\rangle = 0, \qquad \langle\alpha^2\rangle = [\cos^2(\omega) + \cos^2(i)\sin^2(\omega)]/2$$

$$\langle\alpha^4\rangle = 3[\cos^2(\omega) + \cos^2(i)\sin^2(\omega)]^2/8$$

$$\langle\beta^2\rangle = [\sin^2(\omega) + \cos^2(i)\cos^2(\omega)]/2$$

$$\langle\alpha^2\beta^2\rangle = [\cos^2(i)\cos^4(\omega) + 3\cos^2(\omega)\sin^2(\omega) - 4\cos^2(i)\cos^2(\omega)\sin^2(\omega)]/8 + [3\cos^4(i)\cos^2(\omega)\sin^2(\omega) + \cos^2(i)\sin^4(\omega)]/8$$

$$\langle\beta^4\rangle = 3[\cos^2(i)\cos^2(\omega) + \sin^2(\omega)]^2/8, \qquad a' = r'$$

When those identities are applied in expressions (6–8), the results are

$$\langle\langle R_2\rangle\rangle = K_1\{2[3\cos^2(i) - 1] + 3[3\cos^2(i) - 1]e^2 + 15\sin^2(i)e^2\cos(2\omega)\} \tag{12}$$

$$\langle\langle R_3\rangle\rangle = 0 \tag{13}$$

$$\langle\langle R_4\rangle\rangle = K_2\big[C_1 + C_2e^2 + C_3e^2\cos(2\omega) + C_4e^4 + C_5e^4\cos(2\omega) + C_6e^4\cos(4\omega)\big] \tag{14}$$

where

$$K_1 = \frac{\mu' a^2 n'^2}{16}, \qquad K_2 = \frac{9\mu' n'^2 a^4}{65{,}536 a'^2}$$

$$C_1 = 144 + 320\cos(2i) + 560\cos(4i), \qquad C_2 = 5C_1$$

$$C_3 = 1680 + 2240\cos(2i) - 3920\cos(4i), \qquad C_4 = \frac{15}{8}C_1$$

$$C_5 = \frac{C_3}{2}, \qquad C_6 = 4410 - 5880\cos(2i) + 1470\cos(4i)$$

The partial derivatives required for the equations of motion are

$$\frac{\partial R_2}{\partial a} = \frac{\mu' a n'^2}{8}\{2[3\cos^2(i) - 1] + 3[3\cos^2(i) - 1]e^2 + 15\sin^2(i)e^2\cos(2\omega)\} \tag{15}$$

$$\frac{\partial R_2}{\partial e} = 6K_1\{[3\cos^2(i) - 1]e + 5\sin^2(i)e\cos(2\omega)\} \tag{16}$$

$$\frac{\partial R_2}{\partial i} = 3K_1[-2\sin(2i) - 3\sin(2i)e^2 + 5\sin(2i)e^2\cos(2\omega)] \tag{17}$$

$$\frac{\partial R_2}{\partial \omega} = -K_1 30\sin^2(i)e^2\sin(2\omega) \tag{18}$$

$$\frac{\partial R_4}{\partial a} = \frac{9\mu' n'^2 a^3}{16{,}384 a'^2}\big[C_1 + C_2e^2 + C_3e^2\cos(2\omega) + C_4e^4 + C_5e^4\cos(2\omega) + C_6e^4\cos(4\omega)\big] \tag{19}$$

$$\frac{\partial R_4}{\partial e} = 2K_2\left[5C_1e + C_3e\cos(2\omega) + \frac{15}{4}C_1e^3 + C_3e^3\cos(2\omega) + 2C_6e^3\cos(4\omega)\right] \tag{20}$$

$$\frac{\partial R_4}{\partial i} = K_2\big[C_7 + C_8e^2 + C_9e^4 + C_{10}e^2\cos(2\omega) + C_{11}e^4\cos(2\omega) + C_{12}e^4\cos(4\omega)\big] \tag{21}$$

$$\frac{\partial R_4}{\partial \omega} = -K_2\big[2C_3e^2\sin(2\omega) + C_3e^4\sin(2\omega) + 4C_6e^4\sin(4\omega)\big] \tag{22}$$

where

$$C_7 = -640\sin(2i) - 2240\sin(4i)$$

$$C_8 = -3200\sin(2i) - 11{,}200\sin(4i)$$

$$C_9 = -1200\sin(2i) - 4200\sin(4i)$$

$$C_{10} = -4480\sin(2i) + 15{,}680\sin(4i)$$

$$C_{11} = -2240\sin(2i) + 7840\sin(4i)$$

$$C_{12} = 11{,}760\sin(2i) - 5880\sin(4i)$$

The next step is to obtain the equations of motion of the spacecraft. They come from the Lagrange's planetary equations in the form that depends on the derivatives of the disturbing function R with respect to the Keplerian elements.

$$\frac{\mathrm{d}a}{\mathrm{d}t} = 0 \tag{23}$$

$$\frac{\mathrm{d}e}{\mathrm{d}t} = \frac{15\mu' n'^2 e\sqrt{1-e^2}}{8n}\sin^2(i)\sin(2\omega) + f_1(a, e, i, \omega) \tag{24}$$

$$\frac{\mathrm{d}i}{\mathrm{d}t} = \frac{-15\mu' n'^2 e^2}{16n\sqrt{1-e^2}}\sin(2i)\sin(2\omega) + f_2(a, e, i, \omega) \tag{25}$$

$$\frac{\mathrm{d}\omega}{\mathrm{d}t} = \frac{3\mu' n'^2}{8n\sqrt{1-e^2}}[(5\cos^2 i - 1 + e^2) + 5(1 - e^2 - \cos^2 i)\cos(2\omega)] + f_3(a, e, i, \omega) \tag{26}$$

$$\frac{\mathrm{d}\Omega}{\mathrm{d}t} = \frac{3\mu' n'^2\cos i}{8n\sqrt{1-e^2}}[5e^2\cos(2\omega) - 3e^2 - 2] + f_4(a, e, i, \omega) \tag{27}$$

$$\frac{\mathrm{d}M_0}{\mathrm{d}t} = \frac{-\mu' n'^2}{8n}[(3e^2 + 7)(3\cos^2 i - 1) + 15(1 + e^2)\sin^2 i\cos^2\omega] + f_5(a, e, i, \omega) \tag{28}$$

where $f_i(a, e, i, \omega)$ represent the contribution of the fourth-order term. They are given by

$$f_1(a, e, i, \omega) = \frac{9\mu' n'^2 a^2\sqrt{1-e^2}}{65{,}536 a'^2 n}\big[2C_3e\sin(2\omega) + C_3e^3\sin(2\omega) + 4C_6e^3\sin(4\omega)\big] \tag{29}$$

$$f_2(a, e, i, \omega) = -\frac{9\mu' n'^2 a^2\cos(i)}{\sqrt{1-e^2}\,65{,}536 a'^2 n\sin(i)}\big[2C_3e^2\sin(2\omega) + C_3e^4\sin(2\omega) + 4C_6e^4\sin(4\omega)\big] \tag{30}$$

$$f_3(a, e, i, \omega) = \frac{9\mu' n'^2 a^2\sqrt{1-e^2}}{32{,}768 a'^2 n}\left[5C_1 + C_3\cos(2\omega) + \frac{15}{4}C_1e^2 + C_3e^2\cos(2\omega) + 2C_6e^2\cos(4\omega)\right] - \frac{9\mu' n'^2 a^2\cos(i)}{\sqrt{1-e^2}\,65{,}536 a'^2 n\sin(i)}\big[C_7 + C_8e^2 + C_9e^4 + C_{10}e^2\cos(2\omega) + C_{11}e^4\cos(2\omega) + C_{12}e^4\cos(4\omega)\big] \tag{31}$$

$$f_4(a,e,i,\omega) = \frac{9\mu' n'^2 a^2}{\sqrt{1-e^2}\,65{,}536 a'^2 n \sin(i)}\Big[C_7 + C_8 e^2 + C_9 e^4 + C_{10} e^2\cos(2\omega) + C_{11} e^4\cos(2\omega) + C_{12} e^4\cos(4\omega)\Big] \quad (32)$$

$$f_5(a,e,i,\omega) = -\frac{9\mu' n'^2 a^2(1-e^2)}{32{,}768 a'^2 n}\left[5C_1 + C_3\cos(2\omega) + \frac{15}{4}C_1 e^2 + C_3 e^2\cos(2\omega) + 2C_6 e^2\cos(4\omega)\right] - \frac{9\mu' n'^2 a^2}{8192 a'^2 n}\Big[C_1 + C_2 e^2 + C_3 e^2\cos(2\omega) + C_4 e^4 + C_5 e^4\cos(2\omega) + C_6 e^4\cos(4\omega)\Big] \quad (33)$$

There are some conclusions that come directly from the equations of motion:

1) The term μ' is a constant that multiplies all of the equations of motion, and so it is equivalent to a time transformation in the system of the type $\mu' t = t^*$. Thus, all of the results based in those equations are valid for any system of primaries in a proportional timescale. The same is true for the semimajor axis (that is present in the equations in the term n) in the second-order model.

2) The ratio $K_1/K_2 = 4096 a'^2/a^2$ gives an idea of the relative importance of the second- and fourth-order terms. The importance of the fourth-order terms increases when the semimajor axis of the perturbed body increases. This importance also increases with the eccentricity of the perturbed body due to the terms that depend on the eccentricity.

3) The difference between the analytical solutions and the full numerical simulations also increases with those variables. This is confirmed by numerical integrations and by the expansions being made in terms of the eccentricity.

Results

In this section some results are shown related to the third-body perturbation problem. This section is divided in several subsections to show clearly several aspects of the problem.

Circular Orbits and the Critical Inclination

It is possible to identify the existence of circular solutions for both second- and fourth-order models directly from the equations of motion for the averaged models. This means that, in the ideal case of an orbit that starts with zero eccentricity, its eccentricity remains always zero. This occurs because the right-hand side of the equation for the time derivative of the eccentricity is zero. (It is a polynomial in the eccentricity with no independent term.) Another property of those orbits is that the inclination is also constant for the same reason because the time derivative of the inclination is also a polynomial in the eccentricity with no independent term.

The evolutions of these two quantities (eccentricity and inclination) are studied under the fully restricted three-body problem. The results show that the circular solutions with constant inclination do not exist in this more realistic model. The eccentricity oscillates with large amplitude. The inclination remains close to constant most of the time, but from time to time it decreases to the value of the critical inclination, and then it returns to its initial value. The minima in inclination occur at the same time as the maxima in eccentricity. This behavior is similar to the near-circular orbits shown in Figs. 1–4. This result is expected, because there is no physical reason to have a strong difference in the behavior of orbits with eccentricity 0.00 and 0.01. The general conclusion is that the circular solutions with constant inclination appear due to the truncation of the Legendre polynomial and are not physical phenomena, at least for the conditions simulated in this research.

Another important question in this problem is the existence of a critical value for the inclination between the perturbed and the perturbing bodies. This critical inclination is related to the stability of near-circular orbits. The problem is to find under what conditions a spacecraft that starts in a near-circular orbit around the main

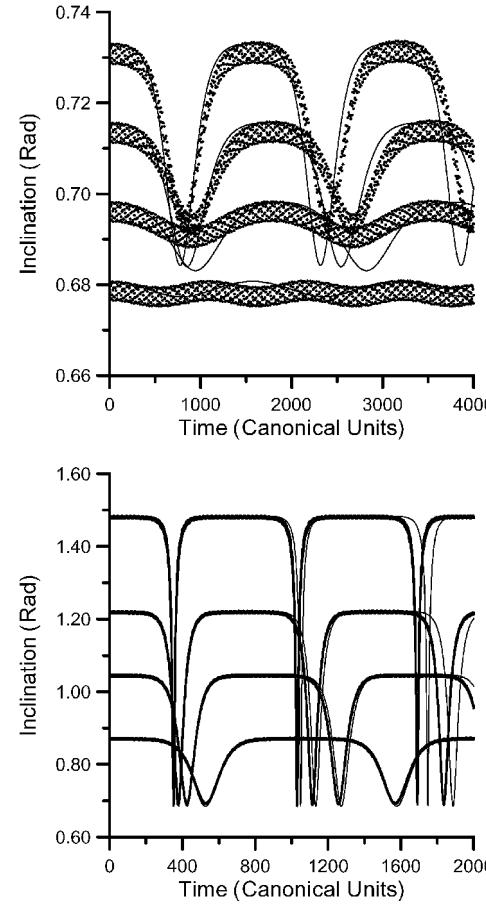

Fig. 1 Time histories for the inclination for a lunar satellite.

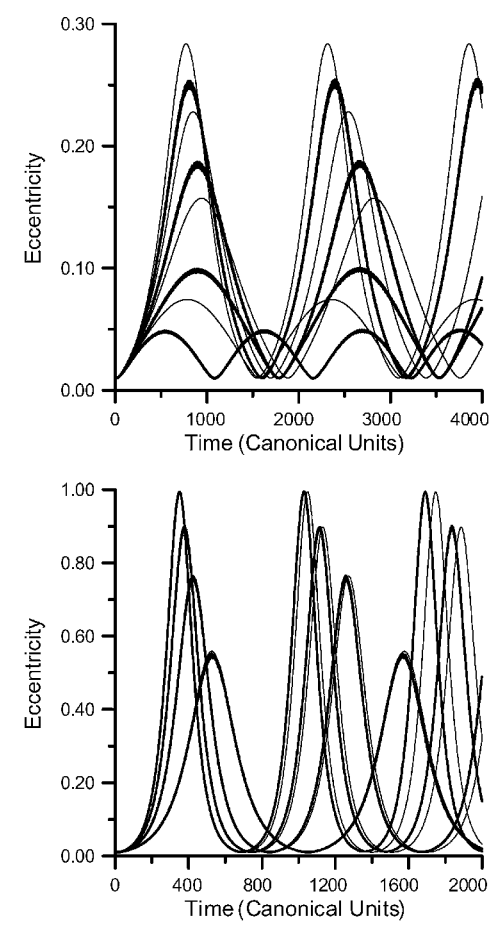

Fig. 2 Time histories for the eccentricity for a lunar satellite.

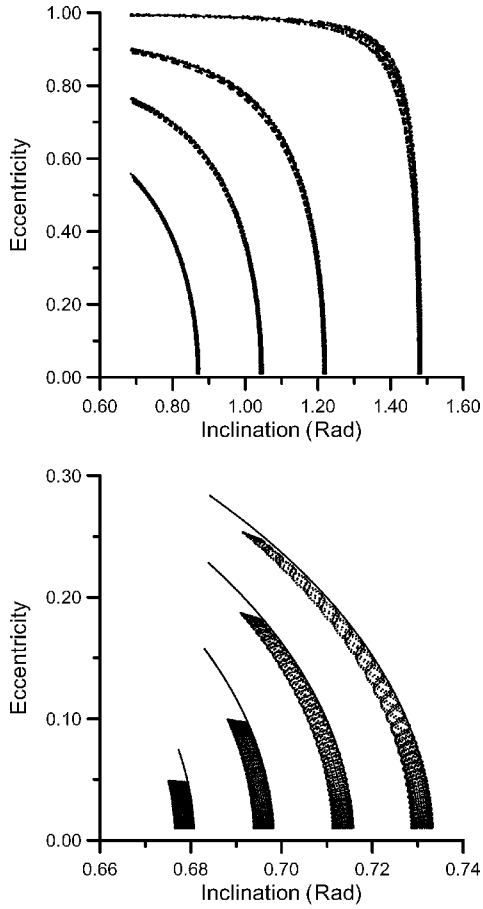

Fig. 3 Inclination and eccentricity for a lunar satellite in the i–e plane.

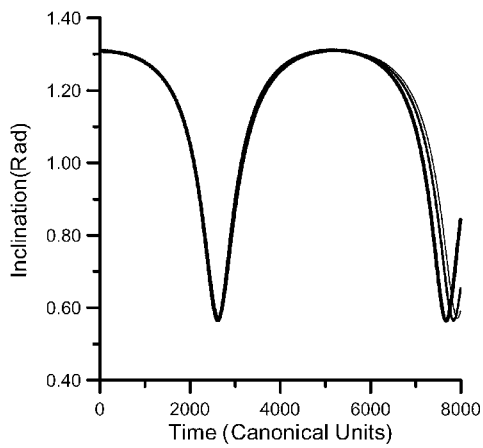

Fig. 4 Comparison between the models: darkest line, numerical; medium line, P4; and thinnest line, P2.

body remains in a near-circular orbit after some time. The answer to this question depends on the initial inclination i_0. There is a specific critical value such that if the inclination is higher than that, the eccentricity increases and the near-circular orbit becomes very elliptic. Alternatively, if the inclination is lower than this critical value, the orbit stays nearly circular. Thus, only orbits with inclinations lower than the critical value are useful for practical purposes. The problem of near-circular orbits is very important because usually a spacecraft that is nominally in circular orbit experiences perturbations from other sources that make its eccentricity become nonzero. In the double-averaged second-order model, this critical value is $i = 39.2315$ deg $[\cos^2(i) = 0.60]$. This critical value also represents the lowest inclination that allows the existence of orbits with eccentricity, inclination, and the argument of periapsis to remain constant under the second-order model. The behavior of the inclination and the eccentricity with time is studied for near-circular orbits covering a large range of initial inclinations ($0 < i_0 \leq 85$ deg) for the mathematical models of orders two and four and the fully restricted three-body problem. For this study, a lunar satellite is used (Figs. 1 and 2). For those simulations, the initial orbits used always have Keplerian elements $a_0 = 0.01$ (3844 km), $e_0 = 0.01$, and $\omega_0 = \Omega_0 = 0$. The initial inclination i_0 varies as shown in Figs. 1 and 2. Remember that the time is defined such that the period of the disturbing body is 2π. In that way, 1000 units of time in Figs. 1 and 2 correspond to about 160 orbits of the disturbing body (in the case of the Earth–moon system). Figures 1 and 2 are divided into two parts only to make the observation of the time evolution easy: values of i_0 in the region of the critical value ($39 < i_0 < 42$ deg) and above the critical value ($i_0 > 50$ deg). The sizes of those regions are chosen to avoid unclear figures due to the different scales involved and are not subject to a detailed study. Figure 1 shows the behavior of the inclination. Figure 2 shows the behavior of the eccentricity, where the higher amplitudes correspond to higher inclinations. In both Figs. 1 and 2, the scattered points (that appear as the darkest line in some plots) represents the results of the fully restricted problem, the thinnest line represents the second-order model, and the intermediate line represents the fourth-order model.

Parts of Figs. 1 and 2 for values of the initial inclination i_0 below the critical angle ($i_0 < 35$ deg) are omitted here, but the results show that the eccentricity oscillates with a very small amplitude (less than 0.025) that increases rapidly when i_0 decreases and the inclination remains constant. For values of i_0 around the critical value ($39 < i_0 < 42$ deg), it is possible to see that the eccentricity oscillates with a larger amplitude (about 0.30) that increases with i_0. The inclination has a very characteristic behavior in this region of i_0. For values of i_0 slightly below the critical angle, the inclination stays close to i_0. For values of i_0 slightly above the critical value, the inclination starts at i_0, decreases until the critical value, and then returns to its original value i_0. Those results show that the critical angle is not a sharp separation between stable and unstable near-circular orbits. For values of i_0 well above the critical value ($i_0 \geq 50$ deg) the eccentricity oscillates with increasing amplitudes that approach 1.0. The inclination keeps its characteristic behavior of starting at i_0, decreasing to the critical value and then returning to its original value i_0. Figures 1 and 2 also show that this behavior repeats itself in an endless cycle. The time required to reach the critical value decreases when i_0 increases. This region has a gradual transition where the eccentricity oscillates with an amplitude that increases quickly with i_0, reaching the value 1.0 only in the case $i_0 = 90$ deg. Figure 3 shows the results in the phase diagram that plots the eccentricity vs the inclination for the regions close to and above the critical value. The region below the critical value shows straight lines and is omitted here. Note that the different scales of the plots show different aspects of the comparison. The comparison between the three models tested shows that the averaged models have smooth curves and that the full model has scattered points, as expected. Because the semimajor axis and eccentricity have low values in those simulations ($a_0 = 0.01$ and $e_0 = 0.01$), the differences between the second- and fourth-order models are not visible in the plots with the scale used. To illustrate better those differences and to justify the development of high-order models, a simulation involving the three models for an Earth satellite is made and shown in Fig. 4. The orbital elements used for this simulation are $a_0 = 0.1$, $e_0 = 0.5$, and $i_0 = 75$ deg. It is clear that the fourth-order model has intermediate results between the second-order and the fully restricted problem. The accuracy of the analytical models decreases with time in a manner that depends on the orbit studied. For higher values of semimajor axis and eccentricity, those differences are even higher.

It is possible to understand those behaviors by examining the second-order equations of motion because the comparisons showed that this model adequately represents the system. The magnitude of the time derivative of the eccentricity is dependent on the term $e\sqrt{(1-e^2)}$, and so it increases when the eccentricity has lower values due to the presence of e. After a value close to 0.71 is reached, however, it starts to decrease due to the term $\sqrt{(1-e^2)}$. Its sign is determined exclusively by $\sin(\omega)$, and it imposes the oscillatory

behavior shown in the plots because ω has a secular variation. For the time derivative of the inclination, the same analysis can be applied. The magnitude is influenced by the term $e^2/\sqrt{(1-e^2)}$, which causes the curious behavior of showing regions of almost constant inclination alternated with sharp decreases and increases. The explanation is that, for lower values of the eccentricity, the term e^2 forces the time derivative to stay close to zero, and the inclination remains almost constant. When the eccentricity increases and reaches values close to 1.0, the term $\sqrt{(1-e^2)}$, present in the denominator, forces the time derivative to increase quickly, tending to infinity, which causes the fast motion of the inclination. The alternation of the sign is caused exclusively by the term $\sin(\omega)$, as explained before. The argument of periapsis has a secular variation because its time derivative is always positive in the situations considered, alternating large regions of slow and short regions of fast increases. The fast increase is also explained by the term $\sqrt{(1-e^2)}$ in the denominator that approaches zero when the eccentricity approaches 1.0.

The practical application of those results is that only near-circular orbits with inclinations lower than the critical value are stable in the long range because above this value the orbit looses its characteristics of near circularity. This is in agreement with the existence of the natural satellites known in the solar system because their inclination is always lower than the critical value. The results are similar to the ones obtained for an Earth satellite,[11,12] taking into account the timescale due to the value of μ'.

Equatorial Orbits

Another property of the second-order system that comes directly from the inspection of the equations of motion is the existence of stable equatorial orbits. This means that if an orbit starts with $i_0 = 0$, the inclination and eccentricity remain constant, and the orbits remain in the equatorial plane. In the second-order model, this property is evident from the equations of motion. If $i_0 = 0$, then the right-hand sides of the expressions for de/dt and di/dt are also zero, because they are proportional to $\sin^2(i)$ and $\sin(2i)$, respectively. For the fourth-order model, the expression for the time derivative for the inclination has a singularity, due to the $\sin(i)$ present in the denominator. The expression for the time derivative of the eccentricity is not zero, because the coefficients C_3 and C_6 that appear in the equation for $f_1(a, e, i, \omega)$ do not vanish when the inclination is zero. The numerical integration of the fully restricted three-body problem model shows the existence of equatorial solutions (zero inclination all of the time) also in this more general model, as expected due to the symmetry of the system. However, in contrast to the second-order model, the eccentricity has short-period oscillations with an amplitude that depends on the initial eccentricity, but it can reach values large enough to destroy completely the circularity of the orbits.

Frozen Orbits

From the equations of motion for the second-order model, it is possible to detect the existence of a family of special orbits that have a constant semimajor axis, eccentricity, inclination, and argument of periapsis called frozen orbits. To obtain this family, it is necessary to find the solutions of the equations $de/dt = di/dt = d\omega/dt = 0$ because the time derivative for the semimajor axis is always zero. To satisfy the equation for the time derivative of the eccentricity, the condition is $\sin(2\omega) = 0$, which implies that $\cos(2\omega) = \pm 1$. When the solution $\cos(2\omega) = +1$ in the equation for the time derivative of the argument of periapsis is analyzed, it is seen that its only possible solution is $e = 1.0$. Thus, only the solution $\cos(2\omega) = -1$ is taken, and it implies that $\omega = 90$ or 270 deg. The vanishing of the time derivative for the inclination does not add any new condition because $\sin(2\omega) = 0$ used earlier implies in $di/dt = 0$. From the equation $d\omega/dt = 0$ and the assumed solution $\cos(2\omega) = -1$, one more condition is found:

$$5\cos^2(i) - 1 + e^2 - 5[1 - e^2 - \cos^2(i)] = 0 \Rightarrow e^2 = 1 - \tfrac{5}{3}\cos^2(i) \tag{34}$$

This is a relation between the eccentricity and the inclination that allows frozen orbits. From this equation, the condition $\cos^2(i) < \frac{3}{5}$ is also obtained. This condition sets a minimum value for the inclination, which is the critical value discussed before, due to the restriction $e^2 > 0$. Those conditions are valid only for the second-order model. When submitted to the fourth-order and to the fully restricted problem model, a frozen orbit is destroyed, and it shows periodic oscillations in all of the three orbital elements. The difference between the fourth-order and the restricted models are in the amplitude of the oscillations. The amplitudes are about 10 times larger when the restricted problem is used. As an example, the frozen orbit with eccentricity 0.3 and inclination 42.36066 deg was simulated, and the oscillations for the fourth-order model were 0.01 rad in inclination, 0.03 in eccentricity, and 0.08 rad in the argument of periapsis. For the restricted model, the oscillations were 0.14 rad in inclination and 0.3 in eccentricity, and the argument of periapsis assumed all values in the interval $[0,\ 2\pi]$ rad. When the equations of motion for the fourth-order model are examined, it is seen that $f_1(a, e, i, \omega) = f_2(a, e, i, \omega) = 0$, but $f_3(a, e, i, \omega) \neq 0$. This means that the eccentricity and the inclination keep their time derivatives null for the fourth-order model. The destruction of the frozen orbits comes from the argument of periapsis because its time derivative is not null, and so the argument of periapsis deviates from the frozen condition. This makes $\sin(2\omega) \neq 0$, and it implies that all of the time derivatives deviate from zero. Another application of the frozen orbits in the second-order model is to test the accuracy of the numerical integration of this model.

Lifetime of Orbits Around Natural Satellites

In this section, the behaviors of orbits around some of the most important natural satellites in the solar system are studied. In all cases, an initial orbit with semimajor axis equal to four times the radius of the satellite is used. The initial eccentricity was varied in the range $0.0 \leq e \leq 0.5$, in steps of 0.05. The initial inclination was varied from 60 to 85 deg, in steps of 5 deg. For each set of initial conditions, the equations of motion given by the restricted problem model were integrated in time until an eccentricity of 0.75 was reached, at which point a collision occurs. Regions with inclination below 60 deg are not included here because they have orbits with eccentricity oscillating below 0.75, as shown in Fig. 1, and they do not crash. The simulations were performed using the three models shown in this paper. The results showed that the second- and the fourth-order models have a strong agreement in all of the cases simulated, but the numerical results agree with the averaged models only for the moon and Charon, which have large values for the mass parameter. Thus, Figure 5 presented here represents the results obtained by the most reliable method permitted in the short times involved: the restricted problem. From several simulations, those times are obtained and plotted in Fig. 5. The horizontal axis represents the initial eccentricity, the vertical axis the initial inclination, and the contour plots are lines of constant lifetime, in sidereal days. Note that the plots for the moon and Europa have two different scales to facilitate the visualization. Table 1 shows the data of the celestial bodies used in the numerical simulations, as obtained from Ref. 13: the period (sidereal days), the mean distance to the planet (10^3 km), the radius of the satellite (kilometers), and the mass parameter (μ), that is, the ratio between the mass of the satellite and the total mass of the system. The numerical integration was performed using a Runge–Kutta 7–8 algorithm. A limit of 3000 canonical units of time, where one canonical unit of time is equal to the period of the satellite around the planet divided by 2π, is included in the simulations. When this time is reached, the numerical integration is stopped, and the collision is assumed not to occur.

Table 1 Data for celestial bodies

Satellite	Sidereal period, days	Mean distance to planet, 10^3 km	Radius of the satellite, km	Mass parameter μ
Moon	27.321661	384.4	1738	0.0121505
Io	1.769137	422	1815	0.0000468
Europa	3.551181	671	1569	0.0000252
Ganymede	7.154552	1070	2631	0.000078
Callisto	16.689018	1883	2400	0.0000566
Titan	15.910290	1221.83	2575	0.000238
Titania	8.705871	435.91	800	0.000068
Triton	5.876843	354.29	1600	0.001298
Charon	6.387100	19.7	600	0.111111

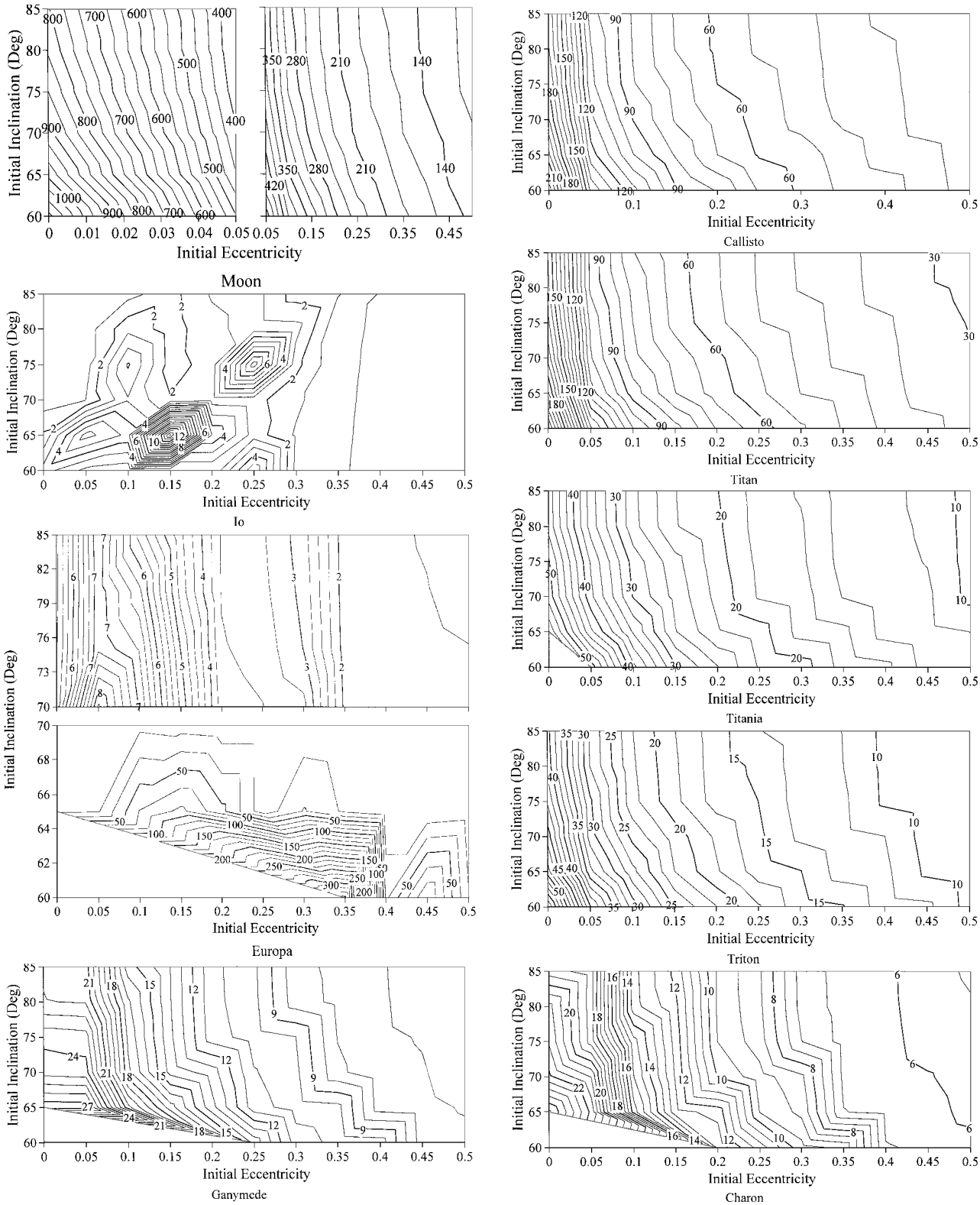

Fig. 5 Lifetime (sidereal days) for orbits around natural satellites.

Looking at the results, some characteristics are evident:

1) For the majority of the cases studied, the dependence on the initial inclination is not strong. The lines of constant time are close to vertical, with a tendency to have a linear decrease in the lifetime of the orbit for higher values of the initial inclination. This result is explained by the range studied for the inclination being above the critical inclination, so that all of the orbits are expected to be unstable.

2) There is a strong, and close to linear, dependence with the initial eccentricity. Detailed studies of the lifetime as a function of the initial eccentricity for several values of the semimajor axis were performed, and the nearly linear relationship was confirmed. The reason for that is that the end of the life of the orbit is reached when the eccentricity has the value 0.75. Thus, when the initial eccentricity is higher, the time to reach the limit value of 0.75 decreases almost linearly.

3) For the Jupiter family, the lifetime decreases when a satellite closer to Jupiter is studied, and so Io has orbits with the shortest lifetimes, usually in the order of few days, and Callisto has the longest ones, ranging from 20 days to more than six months.

4) The mass parameter of the system also plays an important role in this problem. When this parameter increases, the relative value of the mass of the perturbing body decreases, and the lifetimes of the orbits become larger. The moon and Io show this very well. Simulations varying only the mass parameter confirmed this.

Some extra simulations were made to study other details. If a collision occurring when the eccentricity reaches the value 0.75 is neglected and the numerical integration continues beyond this point, the same situation observed for the lunar satellite repeats, and the eccentricity oscillates between the initial value and 1.0. The inclination stays close to its initial value most of the time, but it goes down to the critical value in a periodic motion. The difference from the lunar satellite is only the period of the oscillations, which is much faster in Io, as expected from the second-order analysis made earlier.

Conclusions

This paper develops three mathematical models to study the third-body perturbation: the double average up to second- and fourth-order in the expansion in Legendre polynomials and the fully restricted problem. The results show in detail the behavior of orbits with respect to its initial inclination and the role of the critical inclination in the stability of near-circular orbits. They show that this critical value is a transition region where the eccentricity has an oscillation that increases in amplitude. It has also shown the existence of equatorial solutions (but with the eccentricity oscillating) and the nonexistence of circular solutions under the dynamics given by the restricted three-body problem. The frozen orbits found in the double-averaged second-order model are studied in the fourth-order and the fully restricted models. It is shown that they have their Keplerian elements disturbed by a small periodic oscillation in the fourth-order model and a large periodic oscillation in the restricted problem.

The study of the lifetime of orbits around some natural satellites of the solar system showed the following: 1) The dependence on the initial inclination is not strong, with a tendency to have a linear decrease in the lifetime of the orbit for higher values of the initial inclination. 2) There is a strong and nearly linear dependence with the initial eccentricity. 3) The lifetime decreases when the natural satellite is closer to the planet. 4) When the mass parameter of the system increases, the relative value of the mass of the perturbing body decreases, and the lifetime of the orbits become larger. In general, it is seen that orbits with inclinations higher than 60 deg have a short lifetime.

Acknowledgments

The author is grateful to the National Council for Scientific and Technological Development, Brazil, for Contract 300221/95-9 and to the Foundation to Support Research in São Paulo State (FAPESP) for Contract 1995/9290-1. The author also acknowledges Roger Broucke, whose class notes provided the basis for the double-averaging method.

References

[1]Kozai, Y., "On the Effects of the Sun and the Moon upon the Motion of a Close Earth Satellite," Smithsonian Astrophysical Observatory, Special Rept. 22, Cambridge, MA, 1959.

[2]Musen, P., Bailie, A., and Upton, E., "Development of the Lunar and Solar Perturbations in the Motion of an Artificial Satellite," NASA TN D494, 1961.

[3]Kozai, Y., "Secular Perturbations of Asteroids with High Inclination and Eccentricity," *Astronomical Journal*, Vol. 67, No. 9, 1962, pp. 591–598.

[4]Blitzer, L., "Lunar-Solar Perturbations of an Earth Satellite," *American Journal of Physics*, Vol. 27, No. 9, 1959, pp. 634–645.

[5]Cook, G. E., "Luni-Solar Perturbations of the Orbit of an Earth Satellite," *Geophysical Journal*, Vol. 6, No. 3, 1962, pp. 271–291.

[6]Kaula, M. W., "Development of the Lunar and Solar Disturbing Functions for a Close Satellite," *Astronomical Journal*, Vol. 67, No. 5, 1962, p. 300.

[7]Kozai, Y., "Effects of the Tidal Deformation on the Motion of Satellites," *Publications of the Astronomical Society of Japan*, Vol. 17, No. 3, 1965, pp. 395–402.

[8]Giacaglia, G. E. O., "Lunar Perturbations of Artificial Satellites of the Earth," Smithsonian Astrophysical Observatory, Special Rept. 352, Cambridge, MA, 1973.

[9]Kozai, Y., "A New Method to Compute Lunisolar Perturbations in Satellite Motions," Smithsonian Astrophysical Observatory, Special Rept. 349, Cambridge, MA, 1973.

[10]Hough, M. E., "Orbits Near Critical Inclination, Including Lunisolar Perturbations," *Celestial Mechanics*, Vol. 25, No. 2, 1981, pp. 111–136.

[11]Costa, I. V., and Prado, A. F. B. A., "Orbital Evolution of a Satellite Perturbed by a Third Body," *Advances in Space Dynamics*, edited by A. F. B. A. Prado, National Inst. for Space Research, São José dos Campos, Brazil, 2000, pp. 176–194.

[12]Prado, A. F. B. A., and Costa, I. V., "Third-Body Perturbation in Spacecraft Trajectory," International Astronautical Federation, Paper 98-A.4.05, Sept.–Oct. 1998.

[13]Danby, J. M. A., *Fundamentals of Celestial Mechanics*, 2nd ed., Willman–Bell, Richmond, VA, 1989, pp. 430, 431.